

<https://doi.org/10.33271/nvngu/2024-3/042>

M. Zalyubovskii¹,
orcid.org/0000-0002-9183-2771,
I. Panasyuk²,
orcid.org/0000-0001-6671-4266,
S. Koshel²,
orcid.org/0000-0001-7481-0186,
O. Koshel²,
orcid.org/0009-0006-3788-9298,
L. Akimova³,
orcid.org/0000-0002-2747-2775

1 – Open International University of Human Development
“Ukraine”, Kyiv, Ukraine

2 – Kyiv National University of Technology and Design, Kyiv,
Ukraine

3 – National University of Water and Environmental Engi-
neering, Rivne, Ukraine

* Corresponding author e-mail: markzalubovskiy@gmail.com

SYNTHESIS AND RESEARCH OF THE SPATIAL EIGHT-LINK MECHANISM OF THE BARRELING MACHINE

Purpose. Geometric synthesis of a statically determined spatial eight-link hinged mechanism with rotary kinematic pairs of a barreling machine, in which the working capacity carries out a complex spatial movement, followed by an analytical study of the structural features of the machine mechanism.

Methodology. An analytical approach was used in the study of the eight-link hinged mechanism with rotary kinematic pairs, which consists of geometric and structural synthesis, and the design of barreling machine was modeled in the SolidWorks 2021 automated design software.

Findings. One of the possible options for freeing the spatial mechanism of the barreling machine from passive connection is proposed, the synthesis of a statically determined spatial eight-link hinged mechanism with rotational kinematics is carried out. An appropriate design of a barreling machine with two driving links has been developed, the use of which creates conditions for increasing its reliability during operation and simultaneously increasing the productivity of performing the corresponding barreling operations. Analytical studies of the main geometric and structural parameters of the barreling machine were carried out.

Originality. The connection between the corresponding geometric parameters of the synthesized statically determined spatial eight-link mechanism is established, which allows determining the rational ratio of the lengths of its links to each other. The relationship between the lengths of the links, their position and the angle of swing of the rocker arm together with the drive shaft of the machine is also established.

Practical value. The synthesis of a statically determined spatial eight-link hinged mechanism with rotary kinematic pairs with two degrees of mobility was performed. Based on the synthesis of the mechanism, a new design of the barreling machine with two driving links was developed. Mathematical expressions for calculating the main geometric relationships of the link lengths of the developed machine structure were obtained.

Keywords: *passive connection, statically determined mechanism, rotational kinematic pair, barreling*

Introduction. Spatial mechanisms are widely applied in technological equipment that is used in various industries (chemical and pharmaceutical [1, 2], mining and automotive industry [3], machine building [4, 5], etc.). In their composition such mechanisms can contain various types of kinematic pairs: with several degrees of mobility, for example, spherical or cylindrical, as well as translational and rotational kinematic pairs. In the great majority of spatial mechanisms, a combination of various kinds of kinematic pairs is implemented. The synthesis of such mechanisms is not difficult. But the simplicity of the synthesis is followed by the complexity of manufacturing spherical joints, the need to use anti-friction materials, increased wear of elements of movable links, a short time of use, etc.

Taking into account the above, a more successful variant is the use of spatial mechanisms with rotational kinematic pairs, which are implemented by standard sliding or antifriction bearings. However, it is known [6] that the use in a spatial mechanism of only rotational kinematic pairs is an extremely

problematic aspect from the point of view of the rational synthesis of such mechanisms and their reliable operation. Such mechanisms [7] will be characterized by the structural complexity of their structure.

It is known [3] that the formation of passive connections is possible in the great majority of spatial mechanisms, specifically with rotational kinematic pairs. The presence of a passive connection in the kinematic chain of the spatial mechanism has an extremely negative effect on the operational properties of the corresponding technological equipment, in other cases it makes it impossible to design it in compliance with the necessary technological requirements.

Literature review. A vivid example of such technological equipment is the design of the industrial mixer of bulk fine-dispersed substances “Turbula” [8, 9], which has been put into mass production by the Swiss company “Willy A. Bachofen AG”. It is known [10, 11] that the use of the Turbula mixer made it possible to realize the process of mixing two fractions of bulk fine-dispersed substances in record time, compared to other types of equipment used to implement the same technological processes.

Since 2014, the authors of the article have successfully implemented a mixer for various types of bulk processing of parts [12]: improving surface quality (grinding and polishing), separating parts from sprues, etc. This mixer is based on a spatial mechanism with rotational kinematic pairs with passive linkages. This spatial mechanism with a prototype of the movement of its main link, which corresponds to the movement of an oloid on a plane, was invented in 1929 [13, 14] by the German sculptor and mathematician Paul Schatz.

Previously, it was found that the functioning of such a spatial mechanism is limited by its structural features, in particular, it is able to function only if the necessary ratios of the lengths of its links, which are defined and presented in the works [12, 15]. In addition, the passive connection available in the kinematic chain of the mechanism can cause a number of operational problems, namely: the need to manufacture parts according to tolerances with increased accuracy, the possibility of mechanism jamming caused by a slight deformation of one of its links, etc.

It is known [7, 12] that the use of statically defined “rational”) mechanisms allows one to expand tolerances for the manufacture of parts, reduce labor intensity and cost of manufacturing, and increase the reliability of technological equipment. It is well known [3] that by freeing a spatial mechanism from passive connection, the loads arising in the kinematic pairs of this mechanism will be determined only by dynamic and power technological interactions. Significant works are devoted to the problems of synthesis of “rational” spatial mechanisms [16], including those by the famous scientists L. N. Reshetov “Design of Rational Mechanisms” (1972), and S. N. Kozhevnykov “Fundamentals of Structural Synthesis of Mechanisms” (1979).

Based on the six-link spatial mechanism with the rotating kinematic pairs of the “basic” construction of the industrial mixer of bulk fine-dispersed substances “Turbula”, the authors of the article synthesized several “rational” statically determined spatial mechanisms that allowed expanding significantly the functional purpose of the “basic” construction of the machine like “Turbula”. The designs of the barreling machines that are developed based on the synthesis of statically defined spatial mechanisms have been successfully implemented in domestic production as a result of the signed license agreements between Kyiv National University of Technology and Design and PJSC “Molnii” (Baryshivka), LLC “Poloplast” (Lviv), LLC “Chervonyi Zhovten” (Fastiv) and PJSC “Fakel” (Fastiv), which also demonstrates the perspective of such equipment for today.

Unsolved aspects of the problem. As a result, machines were designed with two operating containers [17], which are kinematically connected to each other. This technical solution allows performing simultaneously two different barreling operations on one machine. However, taking into account the design features of the formed spatial mechanisms, the intensity of movement of the working mass will differ in each individual container, which will lead to different intensity of technological operations, which makes it impossible to complete the technological operation at the same time in both containers of the machine.

Synthesized seven-link spatial mechanisms of machines in which the driven shafts are kinematically connected to the rockers, as well as spatial mechanisms of machines with additional moving links [12, 18], are also known [19]. In one case, the rocker arm has a horizontal axis of rotation, and in the other, a vertical axis. In this way, it is possible to achieve a significant increase in intensity when performing some of the barreling technological operations. However, such structural features of the machines do not have unified features and allow one to perform rationally only some of the barreling technological operations.

The purpose of the article. Taking into account the above, today, an urgent issue is the development of new statically de-

fining spatial mechanisms of the barreling machine, which will simultaneously create conditions for increasing their reliability during operation, increasing the productivity of the relevant barreling technological operations, as well as expanding the sphere of use of such equipment.

Methods. The first part of the article presents the synthesis of an eight-link statically determined spatial mechanism with two degrees of mobility. Due to the release from passive connection, a barreling machine design with complex spatial movement of the working container was developed, which allows regulating the intensity of the corresponding barreling technological operations. In the second part of the article, an analytical study of the spatial mechanism is carried out in terms of calculating the main geometric parameters of the developed barreling machine, which will ensure its rational operation.

In total, well-known methods of synthesis and analysis were used, as well as machine modeling design using SolidWorks 2021 computer-aided design software.

Presentation of the main material and scientific results. Synthesis of an eight-link statically determined spatial mechanism with two degrees of motion. In works [12, 19], a detailed analysis of the spatial six-unit mechanism of the “basic” construction of the Turbula barreling machine with complex spatial movement of the working container was performed. According to the Somov-Malyshev formula, which is used to determine the degree of mobility of spatial mechanisms, it was found that it would be equal to zero. Nevertheless, the barreling machine can function successfully, however, only when ensuring the exact geometric ratios of the lengths of the links between each other, which were previously obtained in works [12, 15]. In practice, it is impossible to manufacture parts with the calculated ideal dimensional accuracy. Thus, the inaccuracy of manufacturing is compensated by the presence of gaps in the kinematic pairs of the spatial mechanism, which, in general, ensures its functioning.

The degree of mobility of such a spatial mechanism, which is equal to zero, is explained by the presence of a passive connection in it. In the introduction, the obvious disadvantages of operating such equipment are indicated.

Taking into account the need to eliminate the passive connection from the kinematic chain of the machine, as well as to create conditions for expanding the sphere of its use by adjusting the intensity of movement of the workpiece inside the container, it was synthesized an eight-link statically defined spatial mechanism.

The kinematic diagram of barreling machine that contains a spatial eight-link mechanism, as well as a model of the corresponding barreling machine (without representation of the drive) is shown in Figs. 1 and 2, respectively.

The spatial mechanism of the machine includes a frame 1, drive 2 located in the frame 1, which consists of an electric motor 3 and a drive shaft 4, as well as an additional drive 5 located in the frame 1, which contains an electric motor 6 and a drive shaft 7. The drive shaft 4 by means of the clutch 8 is rigidly connected to the crank 9, which is mounted in the bearing support 10. The driven shaft 11 is kinematically connected to

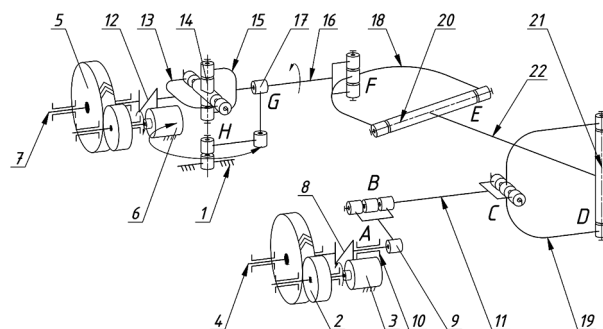


Fig. 1. Kinematic diagram of a barreling machine containing spatial eight-link mechanism

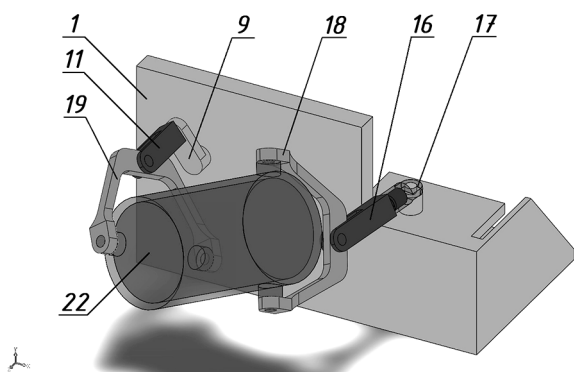


Fig. 2. A model of a barreling machine with two driving links

the crank 9 with the possibility of additional rotation in the vertical plane. The drive shaft 7 by means of the clutch 12 is rigidly connected to the drive fork 13 of the Hook hinge 14. The driven fork 15 of the Hook hinge 14 is rigidly connected to the drive shaft 16, which is kinematically connected to the rocker arm 17 with the possibility of additional oscillatory movement in the horizontal plane. The drive shaft 16 and the driven shaft 11 are pivotally connected to each other by the other ends with the drive fork 18 and the driven fork 19 of the machine, respectively, the diametrically mutually perpendicular axes of which 20 and 21 (Fig. 2) are the axes of fastening of the working container 22. To ensure the functioning of the machine, the vertical axis of rotation of the rocker arm 17 must coincide with the axis of the center of the Hook hinge 14.

Using the Somov-Malyshv formula, it was found that, for a given synthesized mechanism, the degree of mobility will be equal to two

$$W = 6n - \sum_{s=1}^{s=5} (6-s)p_s = 2,$$

where n is the number of movable links (7 links: drive 16 and driven 11 shafts, drive 18 and driven 19 forks, working container 22, crank 9, rocker arm 17); p_s is the number of movable kinematic pairs of s class (8 rotating kinematic pairs: A, B, C, D, E, F, G, H).

In a spatial mechanism with a degree of mobility equal to two, it is necessary to use two driving links, which will allow one to adjust the intensity of movement of the workpiece when moving it between the ends of the container in opposite directions, as well as forming one mode of movement throughout the entire process of machining parts. The driving links of this mechanism will be the drive shaft 16 and the crank 9.

The spatial mechanism of the machine works in the following way. When the additional drive 5 is switched on, the rotational motion from the electric motor 6 is transmitted through the drive shaft 7 and the clutch 12 to the drive fork 13 of the Hook hinge 14. Next, the rotational motion from the drive fork 13 of the Hook hinge 14 is transmitted to the driven fork 15 and the drive shaft 16, which is rigidly connected to the driven fork 15 of the Hook hinge 14. The drive shaft 16, besides the rotational movement, performs an additional oscillatory movement in the horizontal plane together with the rocker arm 17 with which it is kinematically connected. The rotational motion of the drive shaft 16 is transmitted to the drive fork 18 of the machine. The machine drive fork 18 transmits rotation to the working container 22 via axis 20, whereby the latter performs a complex spatial movement and additionally rotates around its own axis. This motion of the container 22 is transmitted through the axis 21 to the driven fork 19 of the machine, from the driven fork 19 to the driven shaft 11, which is kinematically connected to the crank 9, which is installed in the bearing support 10 of the frame 1.

In turn, when the drive 2 is switched on, the rotational motion from the electric motor 3 is transmitted through the

drive shaft 4 and the clutch 8 to the crank 9, which is installed in the bearing support 10 of the frame 1. Such rotation of the crank leads to an additional rotation of the driven shaft 11 in the vertical plane around the axis of the crank. In this way, a part of the working container 22, which is connected to the driven fork 19 of the machine, receives an additional component of spatial movement.

During the performance of the barreling technological operation, depending on the required technological conditions, the drive 2 can be either turned on or off, and the angular speed of rotation of the drive shaft 4 of the drive 2 can differ from the angular speed of rotation of the drive shaft 7 of the additional drive 5.

Due to the fact that the part of the working container 22 connected to the driven fork 19 of the machine will receive an additional component of spatial movement, it appears possible to vary the intensity of movement of the bulk mass between opposite ends of the working container 22. In turn, this will make it possible to bring the intensity of movement of the bulk mass between the opposite ends of the working container 22 in both directions closer to the same, which will create conditions for the implementation of high-intensity barreling technological operations. Further, in §2, we present an analytical study of the synthesized eight-link mechanism with the calculation of the main geometric parameters.

Analytical study of the geometric parameters of the synthesized eight-link mechanism. To begin the analytical study of the eight-link spatial machine mechanism, it is necessary to set the initial data. In particular, it means taking into account the relevant geometric parameters, which are selected depending on the size, type, and number of machined parts, as well as the type of technological operations performed on this equipment and their intensity. So, the interaxial distance of the drive and driven forks is l_F , the interaxial distance of the working capacity is l_{WC} , the crank length is l_C (let us assume that $l_C = 0.4 l_F$), the length of the drive shaft is l_{drive} , the length of the driven shaft is l_{driven} , the length of the rocker arm is l_{rock} .

Moreover $l_{WC} > l_F$ – when this inequality is fulfilled, the machine design, which has a passive connection, loses its functionality.

When operating this mechanism of the barreling machine, at the appropriate position of the crank 9 (shown in Fig. 3), the rocker arm 17, together with the drive shaft 16, will oscillate by an angle δ . During the design of such a machine, an important task is to establish a rational length l_0 , which corresponds to the distance between the horizontal axis of the driven shaft 11 and the vertical axis of rotation of the rocker arm 17, and it is also important to obtain an expression that will allow determining the amplitude of oscillation of the angle δ of the drive shaft 16 depending on changes in the geometric parameters of the machine links. Moreover, for the symmetrical movement of the working container 22 in the vertical plane, the axis of rotation of the crank 9 and the axis of rotation of the rocker arm 17 should be in the same horizontal plane.

For this purpose, let us consider this machine design in the position when the crank 9 is located vertically, while the kinematic pair B “crank-driven shaft” can be located above or below the kinematic pair A “frame-crank”. The horizontal and frontal projections of the machine, which are in projective connection, at this position of the moving links of the machine mechanism are shown in Fig. 3 (the designations in Fig. 3 correspond to the designations in the kinematic diagram – Fig. 1).

Taking into account Fig. 3, the distance l_0 can be determined as follows

$$l_0 = \frac{l_{MAX} + l_{MIN}}{2}, \quad (1)$$

where l_{MAX} is the maximum distance, presented in the horizontal projection, between the axis of rotation of the driven shaft 11 and the center of the kinematic pair F “drive fork – drive shaft”, l_{MIN} is the minimum distance, presented in the horizontal pro-

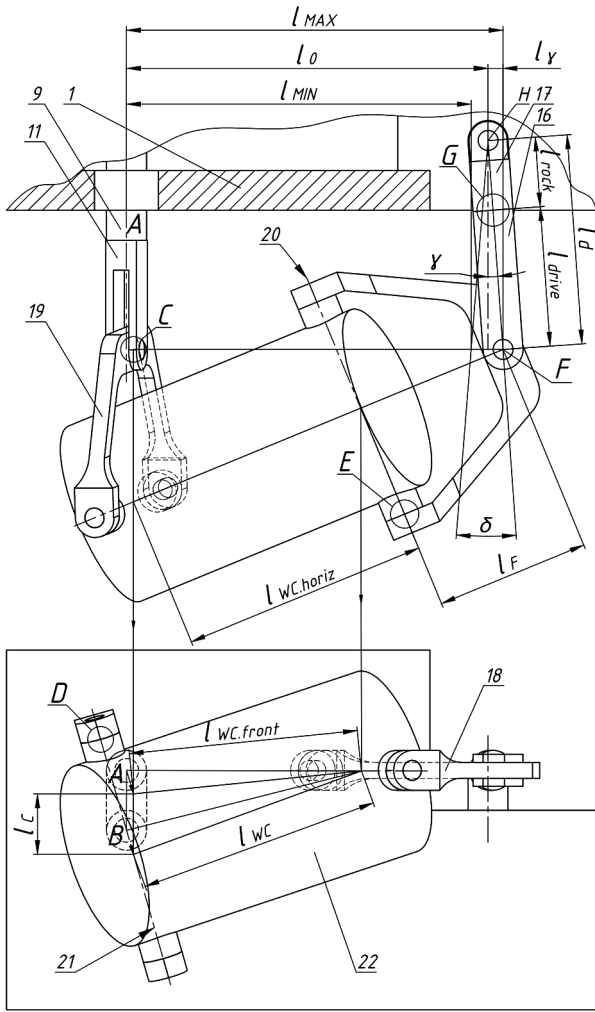


Fig. 3. Horizontal and frontal projections of the machine in projective connection

jection, between the axis of rotation of the driven shaft 11 and the center of the kinematic pair F “drive fork – drive shaft”.

For a similar design of a barreling machine, in works [18, 19], expressions for determining l_{MAX} and l_{MIN} were obtained. The difference is that work [18] investigated the design of a barreling machine that does not have an additional moving link, the crank, and, with a similar position of the moving links, the working capacity was projected onto the horizontal plane in full size. Taking into account the differences in designs, we will write an expression for determining l_{MAX} , taking into account the design features of the studied spatial mechanism of the barreling machine

$$l_{MAX} = \sqrt{(l_F + l_{WC.horiz.})^2 - l_F^2}, \quad (2)$$

where $l_{WC.horiz.}$ is the inter-axial length of the working container in the projection onto the horizontal plane.

In turn

$$\delta = 2 \arcsin \frac{\sqrt{(l_F + \sqrt{l_{WC}^2 - l_C^2})^2 - l_F^2} - \sqrt{l_{WC}^2 + 4(l_F \cos 45^\circ)^2 + l_C^2}}{2 \cdot (l_{rock} + l_{driven})}. \quad (11)$$

Equation (11) allows you to calculate the angle of oscillation δ of the rocker arm 17 with the drive shaft 16 depending on the change in the corresponding geometric parameters of the links.

An important aspect that ensures the functioning of the felting machine is the determination of the maximum permissible interaxial length of the crank $l_{C(MAX)}$, exceeding which will lead to jamming of the mechanism, as well as the possibility of

$$l_{WC.horiz.} = l_{WC.front.}$$

where $l_{WC.front.}$ is the inter-axial length of the working container in the projection on the vertical (frontal) plane.

From the right triangle formed on the frontal projection shown in Fig. 3, we can calculate the length $l_{WC.front.}$, accordingly $l_{WC.horiz.}$

$$l_{WC.horiz.} = l_{WC.front.} = \sqrt{l_{WC}^2 - l_C^2}. \quad (3)$$

We will write expression (2) taking into account (3)

$$l_{MAX} = \sqrt{(l_F + \sqrt{l_{WC}^2 - l_C^2})^2 - l_F^2}. \quad (4)$$

We will adapt the expression presented in [18] to determine l_{MIN} , taking into account the design features of the studied spatial mechanism of the barreling machine

$$l_{MIN} = \sqrt{l_{WC}^2 + 4(l_F \cos 45^\circ)^2 + l_C^2}. \quad (5)$$

Let us write equation (1) with expressions (4 and 5)

$$l_0 = \frac{\sqrt{(l_F + \sqrt{l_{WC}^2 - l_C^2})^2 - l_F^2} + \sqrt{l_{WC}^2 + 4(l_F \cos 45^\circ)^2 + l_C^2}}{2}.$$

The equation makes it possible to calculate the distance l_0 , which will be rational and will correspond to the midpoint of the angle δ of oscillation of the rocker arm 17 with the drive shaft 16.

The magnitude of the oscillation of the angle δ , which depends on the geometric parameters of the machine design, can be calculated as follows

$$\delta = 2\gamma, \quad (6)$$

where γ is the angle of oscillation of the rocker arm when moving from the middle position.

In turn, we write the expression for determining the angle γ

$$\gamma = \arcsin \frac{l_\gamma}{l_d}, \quad (7)$$

where l_γ is difference between distance l_{MAX} (l_{MIN}) and l_0 ; l_d – the total length of the links that perform the oscillatory movement includes the length of the rocker arm $l_{rock.}$, as well as the inter-axial length of the drive shaft $l_{drive.}$

Expression for determining l_d will have the following form

$$l_d = l_{rock} + l_{drive}. \quad (8)$$

It is recommended that the rocker arm with a length $l_{rock.}$, in the position when the driven shaft axis and the drive shaft axis are parallel, does not protrude beyond the machine frame. l_γ is determined as follows

$$l_\gamma = \frac{l_{MAX} - l_{MIN}}{2}. \quad (9)$$

Expression (9) taking into account equations (4 and 5)

$$l_\gamma = \frac{\sqrt{(l_F + \sqrt{l_{WC}^2 - l_C^2})^2 - l_F^2} - \sqrt{l_{WC}^2 + 4(l_F \cos 45^\circ)^2 + l_C^2}}{2}. \quad (10)$$

Let us write expression (6), taking into account equations (7, 8 and 10)

calculating l_C , which depends on other geometric parameters of the machine.

For this purpose, let us consider this machine design in the position when the crank 9 is located horizontally, with its kinematic pair B “crank–driven shaft” located on the left side relative to the kinematic pair A “frame–crank”, and the working capacity 22 is projected onto a horizontal plane in full size. The horizontal projection, with this position of the moving links of the ma-

chine mechanism, is shown in Fig. 4 (designations in Fig. 4 correspond to the designations on the kinematic diagram – Fig. 1).

Analyzing Fig. 4, we can argue that an increase in the inter-axial length l_C will increase the shortest distance l_{DH} between the geometric axis 21 of the working container 22 and the axis of the rocker arm 17, which, in turn, will lead to a decrease in the angles β and θ . It is possible to increase the inter-axial length l_C until the angle α between the axis of the working container 22 and the axis of rotation of the drive shaft 16 is equal to 180° . Thus, the inequality will be reasonable

$$l_{DH} < l_{WC} + l_F + l_d.$$

That is, the maximum allowable length $l_{DH(MAX)}$ will be determined as follows

$$l_{DH(MAX)} = l_{WC} + l_F + l_d. \quad (12)$$

Let us write down the expression for determining the inter-axial length of the crank l_C

$$l_C = \sqrt{l_{DH}^2 - l_{vert}^2} - l_0,$$

where l_{vert} is the vertical component of the distance between the geometric axis 21 of the working container 22 and the axis of the rocker arm 17.

In turn, l_{vert} can be calculated as the sum of the corresponding geometric components of the machine structure, in particular

$$l_{vert} = l_F + l_{driven} + l_{C.vert} + l_{rock}, \quad (13)$$

where l_{driven} is inter-axial length of the driven shaft; $l_{C.vert}$ – crank width.

Taking into account the fact that $l_{vert} = \text{const}$ and $l_0 = \text{const}$, the expression for determining the maximum permissible inter-axial length of the crank $l_{C(MAX)}$, taking into account equation (12), will be as follows

$$l_{C(MAX)} < \sqrt{l_{DH(MAX)}^2 - l_{vert}^2} - l_0.$$

Thus, using expression (13), it is possible to calculate the maximum allowable value of the crank inter-axial length $l_{crank(MAX)}$, exceeding which will lead to jamming of the mechanism.

In general, during the operation of the barreling machine, three positions of the crank 9 can be distinguished, at which the rocker arm 17, together with the drive shaft 16, can be in two extreme positions. Accordingly, for each position of the crank 9, the oscillation angle δ of the rocker arm 17 can be

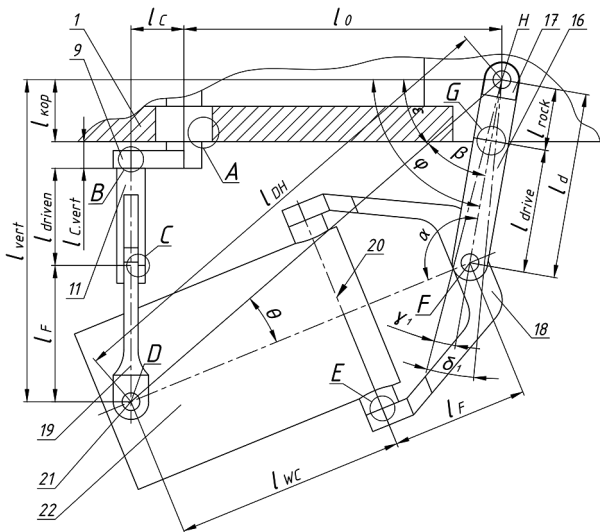


Fig. 4. The position of the moving links, when the rocker arm is in the middle position and the kinematic pair B “crank-driven shaft” is located on the left side relative to the kinematic pair A “frame-crank”

determined. Moreover, this angle of oscillation, at each position of the crank 9, will be different. In particular, such positions of the crank 9 will be:

1. The crank 9 is positioned vertically (kinematic pair B “crank-driven shaft” is located above or below the kinematic pair A “frame-crank”). The position is shown in Fig. 3.

2. The crank 9 is horizontally positioned (the kinematic pair B “crank-driven shaft” is located on the left side relative to the kinematic pair A “frame-crank”). The position is shown in Figs. 5 and 4.

3. The crank 9 is located horizontally (the kinematic pair B “crank-driven shaft” is located on the right side relative to the kinematic pair A “frame-crank”). The position is shown in Figs. 6 and 7.

Earlier, an expression was obtained by which it is possible to calculate the angle δ of rocker arm 17 at the vertical location of the crank 9.

Consider the position of the moving links when the crank 9 is located horizontally (the kinematic pair B “crank-driven shaft” is located on the left side relative to the kinematic pair A “frame-crank”), and the rocker arm 17 is in the extreme right position. This position of the moving links is shown in Fig. 5.

Fig. 5 shows the oscillation angle δ_1 of the rocker arm 17 at the vertical position of the crank 9.

The angle ϕ_1 of inclination of the axis of the rocker arm 17 to the horizontal line can be determined as the sum of the angles β_1 and ε_1 , so

$$\phi_1 = \beta_1 + \varepsilon_1. \quad (14)$$

Based on the geometric construction in Fig. 5, we write the expression for determining the angle ε_1 , as well as the expression for determining the angle β_1

$$\varepsilon_1 = \arctg \varepsilon_1 \frac{l_{driven} + l_{C.vert} + l_{rock}}{l_C + l_0}; \quad (15)$$

$$\beta_1 = \arccos \beta_1 \frac{l_{CH}^2 + (l_F + l_d)^2 - (l_F + l_{WC})^2}{2l_{CH} \cdot (l_F + l_d)}, \quad (16)$$

where l_{CH} is the distance between the geometric centers of the kinematic pairs C “driven shaft – driven fork” and H “frame – rocker arm”. The l_{CH} can be found as follows

$$l_{CH} = \sqrt{(l_C + l_0)^2 + (l_{driven} + l_{C.vert} + l_{rock})^2}. \quad (17)$$

Let us write expression (16) taking into account equation (17)

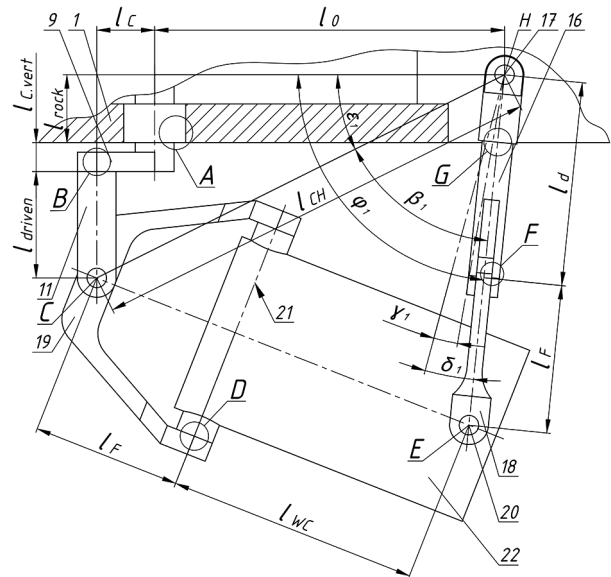


Fig. 5. The position of the moving links, when the rocker arm is in the rightmost position and the kinematic pair B “crank-driven shaft” is located on the left side relative to the kinematic pair A “frame-crank”

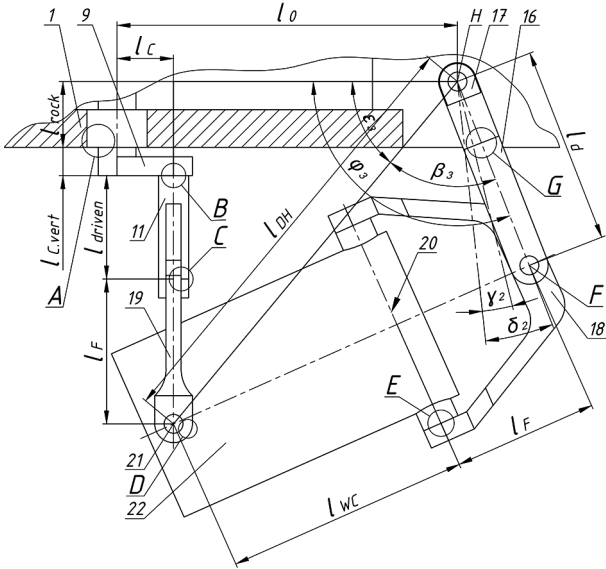


Fig. 6. The position of the moving links, when the rocker arm is in the rightmost position, and the kinematic pair B “crank-driven shaft” is located on the right side relative to the kinematic pair A “frame-crank”

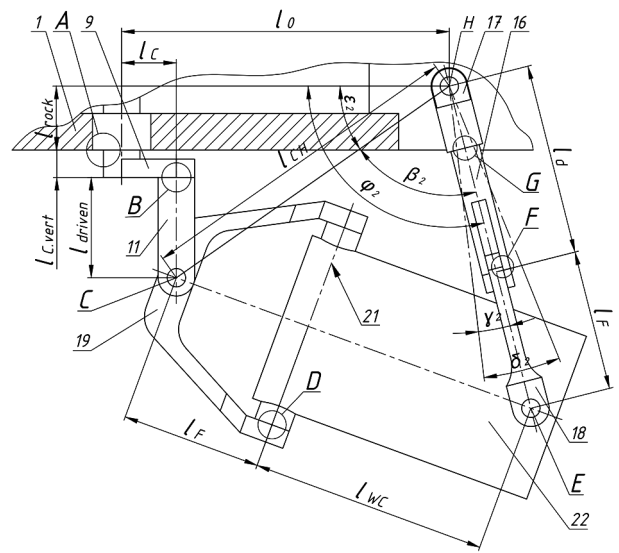


Fig. 7. The position of the moving links, when the rocker arm is in the middle position and the kinematic pair B “crank-driven shaft” is located on the right side relative to the kinematic pair A “frame-crank”

$$\beta_1 = \arccos \beta_1 \frac{(l_C + l_0)^2 + (l_{driven} + l_{C.vert} + l_{rock})^2 + (l_F + l_d)^2 - (l_F + l_{WC})^2}{2\sqrt{(l_C + l_0)^2 + (l_{driven} + l_{C.vert} + l_{rock})^2} \cdot (l_F + l_d)} \quad (18)$$

Let us present expression (14) taking into account (15) and (18)

$$\varphi_1 = \arccos \beta_1 \frac{(l_C + l_0)^2 + (l_{driven} + l_{C.vert} + l_{rock})^2 + (l_F + l_d)^2 - (l_F + l_{WC})^2}{2\sqrt{(l_C + l_0)^2 + (l_{driven} + l_{C.vert} + l_{rock})^2} \cdot (l_F + l_d)} + \arctg \varepsilon_1 \frac{l_{driven} + l_{C.vert} + l_{rock}}{l_C + l_0} \quad (19)$$

Thus, using expression (19), it is possible to determine the maximum angle of inclination φ_1 of the axis of the rocker arm 17 to the horizontal line formed at the corresponding position of the moving links of the machine.

To obtain an expression for calculating the angle δ_1 of oscillation of the rocker arm 17, consider Fig. 4. In Fig. 4, the rocker arm 17 is in the middle position and divides the angle δ_1 in half, so

$$\delta_1 = 2\gamma_1, \quad (20)$$

where γ_1 is half of the angle δ_1 .

The angle γ_1 can be calculated as the difference of angles φ_1 and φ

$$\gamma_1 = \varphi_1 - \varphi. \quad (21)$$

Similarly to (14), an expression can be written to determine the angle φ (Fig. 4) between the horizontal line and the axis of the rocker arm 17 when it is in the middle position relative to the angle δ_1

$$\varphi = \beta + \varepsilon. \quad (22)$$

$$\varphi = \arccos \beta \frac{(l_C + l_0)^2 + (l_F + l_{driven} + l_{C.vert} + l_{rock})^2 + l_d^2 - (l_F + l_{WC})^2}{2\sqrt{(l_C + l_0)^2 + (l_F + l_{driven} + l_{C.vert} + l_{rock})^2} \cdot l_d} + \arctg \varepsilon \frac{l_F + l_{driven} + l_{C.vert} + l_{rock}}{l_C + l_0} \quad (26)$$

Let us write expression (20) taking into account (21), (19), and (26)

$$\delta_1 = 2 \left(\begin{aligned} & \arccos \beta_1 \frac{(l_C + l_0)^2 + (l_{driven} + l_{C.vert} + l_{rock})^2 + (l_F + l_d)^2 - (l_F + l_{WC})^2}{2\sqrt{(l_C + l_0)^2 + (l_{driven} + l_{C.vert} + l_{rock})^2} \cdot (l_F + l_d)} + \arctg \varepsilon_1 \frac{l_{driven} + l_{C.vert} + l_{rock}}{l_C + l_0} - \\ & - \arccos \beta \frac{(l_C + l_0)^2 + (l_F + l_{driven} + l_{C.vert} + l_{rock})^2 + l_d^2 - (l_F + l_{WC})^2}{2\sqrt{(l_C + l_0)^2 + (l_F + l_{driven} + l_{C.vert} + l_{rock})^2} \cdot l_d} - \arctg \varepsilon \frac{l_F + l_{driven} + l_{C.vert} + l_{rock}}{l_C + l_0} \end{aligned} \right) \quad (27)$$

Equation (27), depending on the change in the corresponding geometric parameters of the links, allows us to calculate the oscillation angle δ_1 of the rocker arm 17 together

with the drive shaft 16, which can be formed when the crank 9 is horizontally located, in the case when the kinematic pair B “crank-driven shaft” is located on the left side relative to the

$$\varepsilon = \arctg \varepsilon \frac{l_F + l_{driven} + l_{C.vert} + l_{rock}}{l_C + l_0}; \quad (23)$$

$$\beta = \arccos \beta \frac{l_{DH}^2 + l_d^2 - (l_F + l_{WC})^2}{2l_{Df} \cdot l_d}, \quad (24)$$

where l_{DH} is the distance between the geometric centers of the kinematic pairs D “driven fork – working container” and H “frame – rocker arm”. The distance l_{DH} can be found as follows

$$l_{Df} = \sqrt{(l_C + l_0)^2 + (l_F + l_{driven} + l_{C.vert} + l_{rock})^2}. \quad (25)$$

Let us write expression (24) taking into account equation (25)

$$\beta = \arccos \beta \frac{(l_C + l_0)^2 + (l_F + l_{driven} + l_{C.vert} + l_{rock})^2 + l_d^2 - (l_F + l_{WC})^2}{2\sqrt{(l_C + l_0)^2 + (l_F + l_{driven} + l_{C.vert} + l_{rock})^2} \cdot l_d}$$

Let us substitute (23 and 24) into equation (22)

kinematic pair *A* “frame-crank”.

Let us consider the position of the moving links when the crank *9* is located horizontally (the kinematic pair *B* “crank-driven shaft” is located on the right side relative to the kinematic pair *A* “frame-crank”). The position of the movable links, in which the rocker arm *17* is in the extreme right position, is shown in Fig. 6, and the position of the movable links, in which the rocker arm *17* is in the middle position relative to the oscillation angle δ_2 , is shown in Fig. 7.

Similar to the previous method, the oscillation angle δ_2 of the rocker arm *17* can be calculated as follows

$$\delta_2 = 2\gamma_2, \quad (28)$$

where γ_2 is half of the angle δ_2 .

The angle γ_2 can be calculated as the difference of angles φ_3 and φ_2

$$\gamma_2 = \varphi_3 - \varphi_2. \quad (29)$$

$$\beta_3 = \arccos\beta_3 \frac{(l_0 - l_C)^2 + (l_F + l_{driven} + l_{C.ver} + l_{rock})^2 + l_d^2 - (l_F + l_{WC})^2}{2\sqrt{(l_0 - l_C)^2 + (l_F + l_{driven} + l_{C.ver} + l_{rock})^2} \cdot l_d}. \quad (34)$$

Let us present expression (30) taking into account (32) and (34)

$$\varphi_3 = \arccos\beta_3 \frac{(l_0 - l_C)^2 + (l_F + l_{driven} + l_{C.ver} + l_{rock})^2 + l_d^2 - (l_F + l_{WC})^2}{2\sqrt{(l_0 - l_C)^2 + (l_F + l_{driven} + l_{C.ver} + l_{rock})^2} \cdot l_d} + \arccos\beta_3 \frac{l_{DH}^2 + l_d^2 - (l_F + l_{WC})^2}{2l_{Df} \cdot l_d}. \quad (35)$$

Using expression (35), we can determine the maximum angle of inclination φ_3 of the axis of the rocker arm *17* to the horizontal line formed at the position of the moving links of the machine shown in Fig. 6.

Based on the geometric construction in Fig. 7, we will write the expression for determining the angle φ_2 between the horizontal line and the axis of the rocker arm *17* when it is in the midpoint position relative to the angle δ_2

$$\varphi_2 = \beta_2 + \varepsilon_2. \quad (36)$$

The expressions for determining the angles ε and β will be as follows

$$\beta_2 = \arccos\beta_2 \frac{(l_0 - l_C)^2 + (l_{driven} + l_{C.ver} + l_{rock})^2 + (l_d + l_F)^2 - (l_F + l_{WC})^2}{2\sqrt{(l_0 - l_C)^2 + (l_{driven} + l_{C.ver} + l_{rock})^2} \cdot (l_d + l_F)}. \quad (40)$$

Let us substitute (37 and 40) into equation (36)

$$\varphi_2 = \arccos\beta_2 \frac{(l_0 - l_C)^2 + (l_{driven} + l_{C.ver} + l_{rock})^2 + (l_d + l_F)^2 - (l_F + l_{WC})^2}{2\sqrt{(l_0 - l_C)^2 + (l_{driven} + l_{C.ver} + l_{rock})^2} \cdot (l_d + l_F)} + \arctg\varepsilon_2 \frac{l_{driven} + l_{C.ver} + l_{rock}}{l_0 - l_C}. \quad (41)$$

The resulting expressions (41 and 35) are substituted into equation (28), taking into account expression (29)

$$\delta_2 = 2 \left(\begin{aligned} & \arccos\beta_3 \frac{(l_0 - l_C)^2 + (l_F + l_{driven} + l_{C.ver} + l_{rock})^2 + l_d^2 - (l_F + l_{WC})^2}{2\sqrt{(l_0 - l_C)^2 + (l_F + l_{driven} + l_{C.ver} + l_{rock})^2} \cdot l_d} + \\ & + \arccos\beta_3 \frac{l_{DH}^2 + l_d^2 - (l_F + l_{WC})^2}{2l_{Df} \cdot l_d} - \\ & - \arccos\beta_2 \frac{(l_0 - l_C)^2 + (l_{driven} + l_{C.ver} + l_{rock})^2 + (l_d + l_F)^2 - (l_F + l_{WC})^2}{2\sqrt{(l_0 - l_C)^2 + (l_{driven} + l_{C.ver} + l_{rock})^2} \cdot (l_d + l_F)} - \\ & - \arctg\varepsilon_2 \frac{l_{driven} + l_{C.ver} + l_{rock}}{l_0 - l_C} \end{aligned} \right). \quad (42)$$

Equation (42), depending on the change in the relevant geometric parameters of the links, allows us to calculate the oscillation angle δ_2 of the rocker arm *17*, together with the drive shaft *16*, which can be formed when the crank *9* is horizontal, in the case when the kinematic pair *B* “crank-driven shaft” is located on the right side relative to the kinematic pair *A* “frame-crank”.

Conclusions and prospects for further development. The synthesis of a statically defined spatial eight-link hinge mechanism with rotating kinematic pairs was performed.

Then we write the expression for determining the angle φ_3 (Fig. 6) between the horizontal line and the axis of the rocker arm *17* when it is in the rightmost position

$$\varphi_3 = \beta_3 + \varepsilon_3. \quad (30)$$

Based on the geometric construction in Fig. 6, we write the expression for determining the angle ε_3 , and an expression for determining the angle β_3

$$\varepsilon_3 = \arctg\varepsilon_3 \frac{l_F + l_{driven} + l_{C.ver} + l_{rock}}{l_0 - l_C}; \quad (31)$$

$$\beta_3 = \arccos\beta_3 \frac{l_{DH}^2 + l_d^2 - (l_F + l_{WC})^2}{2l_{Df} \cdot l_d}. \quad (32)$$

The distance l_{DH} can be found as follows

$$l_{Df} = \sqrt{(l_0 - l_C)^2 + (l_F + l_{driven} + l_{C.ver} + l_{rock})^2}. \quad (33)$$

Let us write expression (32) taking into account equation (33)

$$\varepsilon_2 = \arctg\varepsilon_2 \frac{l_{driven} + l_{C.ver} + l_{rock}}{l_0 - l_C}; \quad (37)$$

$$\beta_2 = \arccos\beta_2 \frac{l_{Nf}^2 + (l_d + l_F)^2 - (l_F + l_{WC})^2}{2l_{Nf} \cdot (l_d + l_F)}. \quad (38)$$

Let us find the distance l_{CH}

$$l_{CH} = \sqrt{(l_0 - l_C)^2 + (l_{driven} + l_{C.ver} + l_{rock})^2}. \quad (39)$$

Let us write (38) taking into account equation (39)

Based on the synthesis of the mechanism, a design of a barreling machine is proposed, in which the container performs a complex spatial movement. Such a machine is used for volumetric processing of parts with an abrasive in the form of free granules and mixing of bulk fine-dispersed substances. The developed design of the barreling machine creates conditions for increasing its reliability during operation with a simultaneous increase in the productivity of the corresponding barreling technological operations and allows regulating their intensity.

The mathematical expressions for calculating the basic geometric relationships of the link lengths of the developed machine design were obtained by analytical means. Particularly, the expressions for calculating the rational distance between the axes of rotation of the drive and driven shafts, the expression for determining the maximum permissible interaxial length of the crank, as well as the expressions for calculating the amplitude of oscillation of the rocker arm together with the driven shaft at the corresponding three positions of the crank were obtained. These expressions can be effectively used in the design of barreling equipment with working containers that perform complex spatial motion.

References.

1. Marigo, M., Cairns, D. L., Davies, M., Ingram, A., & Stitt, E. H. (2012). A numerical comparison of mixing efficiencies of solids in a cylindrical vessel subject to a range of motions. *Powder Technology*, 217, 540-547. <https://doi.org/10.1016/j.powtec.2011.11.016>.
2. Jadhav, P. S., & Jadhav, B. R. (2013). A study on mixing of composite solids in the three dimensional turbula mixer. *International Journal of Advanced Engineering Research and Studies*, 2(3), 1-4. E-ISSN2249-8974.
3. Antonyuk, E. Ya., Sakharnov, V. A., & Koval', N. I. (2010). Dynamic System of an Engine with Spatially Rocking Links: a Mathematical Model. *International Applied Mechanics*, 46(9), 1039-1049. <https://doi.org/10.1007/s10778-011-0396-7>.
4. Yarullin, M. G., Isyanov, I. R., & Mudrov, A. P. (2018). Kinematics of angular velocities and accelerated connecting rod (seat) of the simulator. *Kinematika mehanizmov*, 1(37), 24-31. <https://doi.org/10.5862/TMM.37.3>.
5. Evgrafov, A. N., & Petrov, G. N. (2014). Selection of drives of a multi-movement mechanism with redundant inputs. *Nauka i obrazovanie: materialyi 4-y Mezhdunar. nauch.-prakt. konferentsii*, 184-191. ISSN 2223-0807. <https://doi.org/10.1872/MMF-2017-12>.
6. Mudrov, A. G., & Mardanov, R. Sh. (2015). Overview of studies on spatial mechanisms with rotary joints. *Nauchno-metodicheskii zhurnal Teoriya mehanizmov i mashin*, 2(26), 62-70. <https://doi.org/10.5862/TMM.26.7>.
7. Antonyuk, E. Ya., & Zabuga, A. T. (2016). Motion of an Articulated Vehicle with Two-Dimensional Sections Subject to Lateral Obstacles. *International Applied Mechanics*, 52(4), 404-412. <https://doi.org/10.1007/s10778-016-0765-3>.
8. Mayer-Laigle, C., Gatumel, C., & Berthiaux, H. (2015). Mixing dynamics for easy flowing powders in a lab scale Turbula mixer. *Chemical Engineering Research and Design*, (95), 248-261. <https://doi.org/10.1016/j.cherd.2014.11.003>.
9. Marigo, M., Davies, M., Leadbeater, T., Cairns, D.L., Ingram, A., & Stitt, E. H. (2013). Application of Positron Emission Particle Tracking (PEPT) to validate a Discrete Element Method (DEM) model of granular flow and mixing in the Turbula mixer. *International journal of pharmaceuticals*, 446(1-2), 46-58. <https://doi.org/10.1016/j.ijpharm.2013.01.030>.
10. Marigo, M., Cairns, D. L., Davies, M., Cook, M., Ingram, A., & Stitt, E. H. (2010). Developing Mechanistic Understanding of Granular Behaviour in Complex Moving Geometry using the Discrete Element Method. Part A: Measurement and Reconstruction of Turbula-Mixer Motion using Positron Emission Particle Tracking. *CMES: Computer Modeling in Engineering & Sciences*, 59(3), 217-238. <https://doi.org/10.3970/cmcs.2010.059.217>.
11. Marigo, M., Cairns, D. L., Davies, M., Ingram, A., & Stitt, E. H. (2011). Developing Mechanistic Understanding of Granular Behaviour in Complex Moving Geometry using the Discrete Element Method. Part B: Investigation of Flow and Mixing in the Turbula® mixer. *Powder Technology*, 212, 17-24. <https://doi.org/10.1016/j.powtec.2011.04.009>.
12. Zaliubovskiy, M. H., & Panasiuk, I. V. (2022). *Fundamentals of designing machines with complex movement of working capacities for finishing small parts: monograph*. KNUTD. ISBN 978-617-7763-06-1.
13. Schatz, P. (2016). Technik und Verwandlung: Der Weg zu einer menschen- und naturgemäßen Technik. *Verlag am Goetheanum*, 456. ISBN: 978-3-7235-1526-6.
14. Kiran, Bhoite, Kakandikar, G. M., & Nandedkar, V. M. (2015). Schatz Mechanism with 3D-Motion Mixer-A Review. *Materialstoday: proceedings*, 2, 1700-1706. <https://doi.org/10.1016/j.matpr.2015.07.003>.
15. Hrostitskiy, A. A., Evgrafov, A. N., & Tereshin, V. A. (2011). Geometry and kinematics of a spatial hexagon with redundant connections. *Nauchno-tehnicheskie vedomosti SPbGPU*.
16. Serikbay, K., & Algazyi, Zh. (2018). *Parametric synthesis of spatial lever mechanisms: monograph*. Almatyi, KazNTU im. K. I. Satpaeva. ISBN: 978-613-9-82425-0.

17. Zalyubovskii, M. G., & Panasyuk, I. V. (2020). Studying the main design parameters of linkage mechanisms of part-processing machines with two working barrels. *International Applied Mechanics*, 56(6), 762-772. <https://doi.org/10.1007/s10778-021-01053-x>.
18. Zalyubovskiy, M. G., Panasyuk, I. V., Koshel', S. O., & Koshel', G. V. (2021). Synthesis and analysis of redundant-free seven-link spatial mechanisms of part processing machine. *International Applied Mechanics*, 57(4), 466-476. <https://doi.org/10.1007/s10778-021-01098-y>.
19. Zalyubovskii, M. G., & Panasyuk, I. V. (2020). On the study of the basic design parameters of a seven-link Spatial mechanism of a part processing machine. *International Applied Mechanics*, 56(1), 54-64. <https://doi.org/10.1007/s10778-020-00996-x>.

Синтез та дослідження просторового восьмиланкового механізму галтувальної машини

М. Г. Залюбовський^{*1}, І. В. Панасюк², С. О. Кошель²,
О. С. Кошель², Л. М. Акімова³

1 – Відкритий міжнародний університет розвитку людини «Україна», м. Київ, Україна

2 – Київський національний університет технологій та дизайну, м. Київ, Україна

3 – Національний університет водного господарства та природокористування, м. Рівне, Україна

* Автор-кореспондент e-mail: markzalubovskiy@gmail.com

Мета. Геометричний синтез статично визначеного просторового восьмиланкового шарнірного механізму з обертальними кінематичними парами галтувальної машини, в якій робоча ємність здійснює складний просторовий рух, із подальшим аналітичним дослідженням конструктивних особливостей механізму машини.

Методика. Був використаний аналітичний підхід при дослідженні восьмиланкового шарнірного механізму з обертальними кінематичними парами, що полягає в геометричному та структурному синтезі, здійснене моделювання конструкції даної галтувальної машини в програмному забезпеченні автоматизованого проектування SolidWorks 2021.

Результати. Запропоновано один із можливих варіантів звільнення просторового механізму галтувальної машини від пасивного зв'язку, здійснено синтез статично визначеного просторового восьмиланкового шарнірного механізму з обертальними кінематичними парами. Розроблена відповідна конструкція галтувальної машини з двома ведучими ланками, використання якої створює умови для підвищення її надійності під час експлуатації та одночасного збільшення продуктивності виконання відповідних галтувальних операцій. Аналітичним шляхом виконані дослідження основних геометричних і конструктивних параметрів галтувальної машини.

Наукова новизна. Установлено зв'язок між відповідними геометричними параметрами синтезованого статично визначеного просторового восьмиланкового механізму, що дозволяє визначити раціональні відношення довжин його ланок між собою. Також установлено взаємозв'язок між довжинами ланок, їх положенням і кутом коливання коромисла разом із ведучим валом машини.

Практична значимість. Виконано синтез статично визначеного просторового восьмиланкового шарнірного механізму з обертальними кінематичними парами із двома ступенями рухомості. На основі синтезу механізму розроблена нова конструкція галтувальної машини із двома ведучими ланками. Отримані математичні вирази для розрахунку основних геометричних взаємозв'язків довжин ланок розробленої конструкції машини.

Ключові слова: пасивний зв'язок, статично визначений механізм, обертальна кінематична пара, галтування

The manuscript was submitted 28.01.24.

ЗМІСТ

Розробка родовищ корисних копалин	5
Є. А. Коровяка, Є. М. Ставичний, О. Б. Марцинків, А. О. Ігнатів, А. В. Яворський. Вивчення особливостей залягання та шляхи підвищення якості розмежування продуктивних горизонтів вуглеводнів	5
Г. Махгалі, А. Хафсауї, З. Мездуд, А. Буслама, А. Ідрес. Оптимальні параметри вибухового руйнування в умовах кар'єру Бен Азуз на основі досліджень міцності вапнякової породи	12
Ч. В. Фам, Л. К. Нгуєн, К. С. Цао, К. В. Ле, Т. Г. Нгуєн, Х. Т. Т. Ле. Використання стандарту CityGML для 3D ГІС підземних і відкритих гірничих виробок	19
З. Маланчук, В. Мошинський, В. Лозинський, В. Корнієнко, В. С. Сорока. Визначення технологічних параметрів гідромеханічного видобутку бурштину в Поліському регіоні України	27
Фізика твердого тіла, збагачення корисних копалин	35
М. Р. Шаутенов, А. Бегалінов, Н. Т. Акказіна. Переробка рідкісноземельної руди кори вивітрювання	35
Геотехнічна і гірничая механіка, машинобудування	42
М. Г. Залобовський, І. В. Панасюк, С. О. Кошель, О. С. Кошель, Л. М. Акімова. Синтез та дослідження просторового восьмиланкового механізму галтувальної машини	42
В. М. Афонін, О. І. Воронков, А. М. Авраменко, А. С. Птушка, Д. О. Протектор. Вплив багатофазного впорскування палива на техніко-економічні показники транспортного дизельного двигуна	50
О. М. Хорєв, О. В. Линник, П. О. Коротаєв, Ю. А. Биков, Є. С. Агібалов. Вплив колових навалів лопатей робочих коліс насос-турбін на енергетичні характеристики	56
О. В. Панченко, К. С. Заболотний. Розрахунок довговічності зварних з'єднань у механізмі тюбінгоукладача з використанням цифрових методів	63
І. Ф. Альєрефо, М. О. Равашдех, О. Є. Мацулевич, О. О. Вершков, С. В. Галько, О. М. Супрун. Проектування функціональних поверхонь кулачків розподільчого валу двигунів внутрішнього згоряння	72
Електротехнічні комплекси та системи	79
До Нху И, Трінг Б'єн Туй, Ле Ань Туан, Нго Сюан Куонг. Конфігурація ротора для покращення робочих характеристик СДПМЛП у гірничодобувній галузі	79
Екологічна безпека, охорона праці	87
В. А. Цопа, О. О. Яворська, С. І. Чеберячко, О. В. Дерюгін, М. С. Брезіцька. Розробка концепції з удосконалення системи управління безпекою праці і здоров'ям працівників в Україні	87
О. Мансурі, С. Бердуді, Н. Хуссу, А. Буслама, У. Херфан. Вплив затверділих відходів цементу та свіжого цементу на обробку набухаючого ґрунту	95
І. М. Кочмар, В. В. Карабин, В. М. Кордан. Еколого-геохімічні аспекти термічного впливу на аргіліти відвалів Львівсько-Волинського кам'яновугільного басейну	100
А. А. Макурін, О. В. Усатенко, Н. Л. Шишкова. Сучасні інструменти управління декарбонізацією України на державному й локальному рівнях	108
І. В. Єфімова, О. В. Смирнова, Т. Г. Шендрік. Антиоксидантні властивості буровугільних гумінових речовин	116
О. Назаренко, А. Березовська, В. Тимошук, Є. Шерстюк. Інтегрована система моніторингу водних ресурсів у структурі екологічної безпеки півдня України	122
В. П. Щокін, А. В. Павличенко, В. В. Єжов, М. В. Кормер. Екологічна ефективність гуматового реагенту у внутрішніх і зовнішніх гідрозабійках кар'єрів	128
Інформаційні технології, системний аналіз та керування	135
О. Лактіонов, І. Лактіонова. Удосконалення методу оптимізації прогнозування ефективності робототехнічної платформи	135
Р. С. Ситник, Вік. В. Гнатушенко. Управління потоками даних в інформаційних системах із використанням технології блокчейн	142

С. А. Золотарьова, М. С. Пономарьова, В. Є. Новікова, С. В. Станкевич, А. П. Золотарьов. Інтеграція навчального процесу у вищій школі із цифровими технологіями	149
Б. Б. Імансакіпова, І. В. Васильєв, Ш. К. Айтказінова, М. М. Каліпанов, К. Ж. Ісабаєв. Ідентифікація та пригнічення сигналів задньої пелюстки діаграми спрямованості антени радара	157
Економіка та управління	163
А. В. Бессонова, М. В. Белобородова, Л. С. Безугла, А. В. Кулінська, О. М. Ащеулова. Кадровий потенціал промислових підприємств: формування та управління	163
С. О. Доцюк, І. А. Чіков, О. М. Шевченко, В. С. Ніценко, Н. А. Герасимчук, М. М. Демидова. Оцінка інституційного розвитку інноваційної діяльності для забезпечення економіки держави	171
Л. Г. Соляник, Н. М. Штефан, Д. С. Букреєва. Фінансова детермінанта повоєнної відбудови національної економіки на принципах європейського «зеленого» курсу	181
С. А. Яремко, Р. М. Новицький, Л. М. Радзіховська, Л. В. Бондарчук. Автоматизація побудови індивідуальної освітньої траєкторії здобувача вищої освіти	191
Р. О. Мовчан, О. О. Дудоров, Д. В. Каменський, А. А. Вознюк, Т. П. Макаренко. Кримінальна відповідальність за незаконні дії з бурштином: правотворчі та правозастосовні проблеми.	197
Т. В. Капелюшна, С. В. Легомінова, А. Ю. Голобородько, Ю. М. Лисецький, Т. І. Носова. Методологічні підходи до управління безпекою підприємства: традиційні та трансформовані до умов функціонування	204